JOURNAL OF VIROLOGY, May 1985, p. 392–400
0022-538X/85/050392-09$02.00/0

Vol. 54, No. 2

Temporal Regulation of Baculovirus RNA: Overlapping Early and Late Transcripts†

PAUL D. FRIESEN AND LOIS K. MILLER*

Department of Bacteriology and Biochemistry, University of Idaho, Moscow, Idaho 83843

Received 1 November 1984/Accepted 11 January 1985

Analysis of the temporal sequence of RNA transcription within the *Autographa californica* nuclear polyhedrosis virus genome revealed individual transcription units composed of overlapping early or late RNAs, or both. High-resolution S1 nuclease mapping within the 3.0-kilobase *Hin*dIII-K fragment located five overlapping RNAs (1.07, 1.38, 2.63, 3.16, and 3.50 kilobases) transcribed in the same direction and terminated at a common 3′ site. The smallest RNAs appeared early but were replaced in time by successively larger RNAs initiated further upstream. Primer extension analysis supported the contention that this temporal regulation involved the sequential activation of upstream promoters and the coordinate deactivation of downstream promoters. As such, transcription from upstream genes may suppress that of downstream genes via transcriptional interference (promoter occlusion) and thereby facilitate sequential expression of different viral functions. In contrast, overlapping RNAs with extended 3′ ends were transcribed from the abundantly expressed p10 and polyhedrin genes mapping to the *Hin*dIII-Q,P/*Eco*RI-P and *Hin*dIII-V/*Eco*RI-I fragments, respectively. These RNAs were synthesized maximally during the very late occlusion phase and consisted of a major small transcript and several larger but less abundant transcripts.

Expression of the large (ca. 128-kilobase [kb]) circular DNA genome of *Autographa californica* nuclear polyhedrosis virus (AcNPV), an insect baculovirus, involves a complex cascade of regulatory events culminating in an unusual biphasic production of two infectious forms of virus: extracellular nonoccluded virus, followed later by occluded virus composed of multiple virions embedded within polyhedral inclusion particles. The complexity of this regulatory pathway is evidenced by the sequential and, in most cases, transient synthesis of a large number of viral polypeptides (5, 7, 23, 29, 39). Accordingly, viral protein synthesis has been divided into four phases: immediate early α (2 h postinfection), early β (6 h), which defines the onset of viral DNA synthesis, late γ (10 to 12 h), and very late δ (15 h and on), associated with the viral occlusion process. Except for immediate early α, each class appears to require the proper expression of proteins of the preceding class (16, 17, 27).

It remains to be shown that regulation of AcNPV protein synthesis occurs at the level of transcription. Early transcription occurs at dispersed regions of the genome, and as infection proceeds most of the genome is transcribed (8). Several early and many late genes have been mapped to the AcNPV genome by in vitro translation of hybrid-selected RNA (1, 9, 19, 30); however, only one of these genes has been assigned a function, polyhedrin (28,872 daltons), which represents the major protein component of viral occlusion particles. The intracellular abundance of polyhedrin and another viral protein of unknown function, p10, is correlated with the copious amounts of their respective mRNAs found late in infection (1, 29, 31).

To investigate the mechanisms involved in the regulation of AcNPV gene expression, we have hybridized recombinant clones of small genomic restriction fragments or cDNA clones of viral mRNA to Northern blots of polyadenylated [poly(A)$^+$] RNA isolated from cells at intervals after infection. This has enabled us to identify various temporal patterns of overlapping RNAs and thereby further analyze the organization of both early and late transcription units.

We report here that, within several regions of the AcNPV genome, RNA transcription is under strict temporal control. Thus, regulation at the level of transcription is responsible in part for the synthesis of various temporal classes of viral proteins. Two types of transcriptional units were identified. The first was composed of overlapping early and late RNAs with a common 3′ end. This type of organization has important implications for the coordinate regulation of early and late transcripts. The second type was composed of abundant overlapping RNAs with extended 3′ ends. These RNAs were transcribed maximally during the late occlusion (δ) phase and included the polyhedrin and p10 mRNAs.

MATERIALS AND METHODS

Cells and virus infection. *Spodoptera frugiperda* IPLB-SF-21 cells (34) were propagated in TC100 medium (GIBCO Laboratories, Grand Island, N.Y.) (11) supplemented with 2.5 mg of tryptose broth per ml and 10% fetal bovine serum (K.C. Biologicals, Lenexa, Kans.). Cell monolayers (2×10^7 cells per 100-mm plate) were inoculated with extracellular AcNPV L-1 (18) at a multiplicity of 20 PFU per cell. After a 1-h adsorption at room temperature, the residual inoculum was removed and the monolayers were washed twice with TC100. Fresh growth medium (6 ml) was added, and incubation was continued at 27°C. Time zero was defined as the point at which the viral inoculum was removed.

RNA isolation. Cells were harvested at 2, 6, 12, and 24 h after infection by scraping the plates with a rubber policeman. The pooled cells were collected by low-speed ($400 \times g$) centrifugation, washed twice with ice-cold phosphate-buffered saline (18), and resuspended in ice-cold TNM buffer (30 mM Tris-hydrochloride [pH 7.6], 0.1 M NaCl, 10 mM $MgCl_2$). Nonidet P-40 was added to a final concentration of 0.75%, and after a 5-min incubation on ice, the suspension was clarified by centrifugation at $12,000 \times g$ for 6 min (0°C). The resulting cytoplasmic supernatant was made 25 mM in

* Corresponding author.

† Research paper no. 84512 of the Idaho Agricultural Experiment Station.

EDTA and 0.1% in sodium dodecyl sulfate (SDS) and then extracted twice with phenol (1 volume) and chloroform (1/2 volume) containing 0.1% β-hydroxyquinoline. The RNA-containing phase was extracted once with 1 volume of chloroform and precipitated overnight (−20°C) with 2 volumes of absolute ethanol.

Poly(A)$^+$ RNA was selected by the method of Hruby and Roberts (15). In brief, total cytoplasmic RNA from 10^8 infected cells in 10 mM Tris-hydrochloride (pH 7.5)–0.5 M NaCl–1 mM EDTA–0.2% SDS was heated to 65°C for 5 min, cooled quickly on ice, and applied to a 1-ml column of oligodeoxythymidylic acid-cellulose (Bethesda Research Laboratories, Bethesda, Md.) equilibrated with the same buffer. After the column was washed, the bound RNA was eluted with 10 mM Tris-hydrochloride (pH 7.5)–1 mM EDTA–0.2% SDS. Yields of poly(A)-containing RNA from 10^8 cells harvested 12 h after infection were routinely 40 to 50 μg (A_{260} of 1.25).

Gel electrophoresis and hybridization analysis of RNA. Poly(A)-containing RNA (2 to 5 μg per lane) was denatured by glyoxalation (24) and subjected to electrophoresis on horizontal 1.7% agarose gels (18 by 15 by 0.6 cm) in 10 mM sodium phosphate (pH 7.0)–1 mM EDTA. The RNA was transferred to nitrocellulose (BA-85; Schleicher and Schuell, Inc., Keene, N.H.) with 20× SSC (1× SSC is 0.15 M NaCl plus 0.015 M trisodium citrate). The procedures for transfer and hybridization were essentially those of Thomas (33). RNA blots were prehybridized for 15 to 20 h at 42°C in 50% formamide–5× SSC–50 mM sodium phosphate (pH 7.0)–5× Denhardt reagent (1× is 0.2% each of bovine serum albumin, Ficoll, and polyvinylpyrrolidine)–0.1% SDS–100 μg of sheared, denatured salmon sperm DNA per ml. Hybridization was conducted for 24 to 36 h at 42°C with the same mixture, except that the Denhardt reagent was reduced to 1× and 10% dextran sulfate was included.

Radiolabeled DNA probes were prepared by nick translation with [α-^{32}P]dCTP (3,000 Ci/mmol; New England Nuclear Corp., Boston, Mass.) and *Escherichia coli* DNA polymerase (Bethesda Research Laboratories) (25). Probes with specific activities of 2×10^8 to 5×10^8 cpm/μg were denatured by heating for 5 min (100°C), quickly cooled on ice, and then added to a final concentration of 2.5 ng/ml of the above hybridization mixture. RNA blots were washed in 2× SSC–0.1% SDS at room temperature and then in 0.1× SSC–0.1% SDS at 50°C as described previously (33); they were then exposed to Kodak XAR5 film with the aid of Du Pont Cronex intensifying screens.

Recombinant plasmids. Hybrid pBR322 plasmids containing DNA complementary to AcNPV poly(A)-containing RNA isolated late in the infection (27 h) were constructed previously (1). The cDNA clones (pMA) are designated by the letters of the viral restriction fragments (*Hin*dIII, *Eco*RI, and *Sst*I, respectively) to which they were homologous by using adopted AcNPV nomenclature (36). The map coordinates for each cDNA plasmid were verified as described previously (1). The AcNPV *Hin*dIII-K and -Q restriction fragments and FP-DS *Hin*dIII-K subfragments (26) were cloned by using plasmids pBR322 and pUC8 (35) as vectors. Recombinant plasmids were propagated in the JM83 strain of *E. coli* and plasmid DNA was isolated by the lysis-by-boiling method (13) described by Maniatis et al. (22).

S1 nuclease mapping of AcNPV RNA. The 5′ and 3′ ends of viral transcripts were mapped by the S1 nuclease procedure of Berk and Sharp (4) as modified by Weaver and Weissman (38). 5′-End-labeled probes were generated by cleaving appropriate AcNPV recombinant clones at the desired site with a single enzyme. The 5′ ends were dephosphorylated with calf intestinal phosphatase (Sigma Chemical Co., St. Louis, Mo.) and radiolabeled with T4 polynucleotide kinase (Bethesda Research Laboratories) and [γ-^{32}P]ATP (3,000 Ci/mmol; New England Nuclear) (22). The DNA was then cleaved with a second restriction enzyme to yield fragments radiolabeled exclusively at one position. These fragments were purified by agarose gel electrophoresis. 3′-Specific S1 probes were radiolabeled at a single 3′ end in a similar manner by using T4 polymerase (Bethesda Research Laboratories) and [α-^{32}P]dCTP (3,000 Ci/mmol) (22). Specific activities of these probes were 5×10^5 to 8×10^5 cpm/μg.

DNA-RNA hybridizations consisting of 2 μg of poly(A)$^+$-selected cell RNA and 50 to 150 ng of probe DNA were conducted in 30 μl of 80% formamide–40 mM PIPES [piperazine-*N*,*N*′-bis(2-ethanesulfonic acid)] (pH 6.4)–0.4 M NaCl–1 mM EDTA for 4 h. Optimum hybridization temperatures (42 or 50°C) were determined empirically. Samples were diluted 10-fold into S1 buffer (5 mM sodium acetate [pH 4.6], 4.5 mM $ZnSO_4$, 0.28 M NaCl, 5% glycerol, 20 μg of denatured salmon sperm DNA per ml) containing 500 U of S1 nuclease (Bethesda Research Laboratories) per ml and then incubated at 37°C for 30 min. The S1 hybrids were precipitated with ethanol, denatured, and analyzed by electrophoresis on 4% polyacrylamide–7 M urea–TBE (89 mM Tris-hydrochloride [pH 8.3], 89 mM boric acid, 2 mM EDTA) gels. Size standards were derived from *Taq*I or *Hpa*II digests of plasmid pUC19 (35) which were 3′ end labeled as described above.

Primer extension analysis. A 390-base-pair (bp) *Hpa*II-*Hin*dIII primer derived from the rightmost portion of the *Hin*dIII-K fragment (see Fig. 6) was 5′ end labeled exclusively at the *Hin*dIII site by using procedures described above. The primer (5 ng, 10^6 cpm/μg) was annealed to 2 μg of poly(A)-selected RNA by using hybridization conditions for S1 nuclease analysis described above. The primer-RNA hybrids were diluted 10-fold with 0.2 M sodium acetate (pH 5.2), precipitated with ethanol, and redissolved in 50 μl of reverse transcriptase buffer (0.1 M Tris-hydrochloride [pH 8.3], 10 mM dithiothreitol, 50 mM KCl, 10 mM $MgCl_2$, 50 μg of actinomycin D [P-L Biochemicals, Inc., Milwaukee, Wis.] per ml, 1 mM each of the four deoxyribonucleotides, vanadyl ribonucleoside complex). Reverse transcriptase (Bethesda Research Laboratories) was added to a concentration of 600 U/ml. The reaction was carried out under incubation at 42°C for 1 h and then terminated with 25 mM EDTA. The products were precipitated with ethanol, denatured, and resolved by electrophoresis on 4% polyacrylamide–7 M urea–TBE gels.

RESULTS

Temporal regulation of transcription in the *Hin*dIII-K region of AcNPV. The temporal sequence of RNAs transcribed from various regions of the AcNPV genome was examined by hybridizing Northern blots of poly(A)$^+$ RNA with recombinant clones of viral restriction fragments or clones of DNA complementary to viral mRNA (see below). Such analyses revealed a dramatic example of temporal regulation of early and late RNAs transcribed within the *Hin*dIII-K region located between 85.1 and 87.5 map units of the AcNPV genome (Fig. 1). Three temporal classes of RNA were identified on the basis of the time of their maximum synthesis: α (2 h), consisting of two transcripts (1.07 and 1.38 kb), β (6 h), consisting of one transcript (2.63 kb), and γ (12 h), consisting of two transcripts (3.16 and 3.50 kb) plus several others (4 kb and larger). Regulation involved the sequential

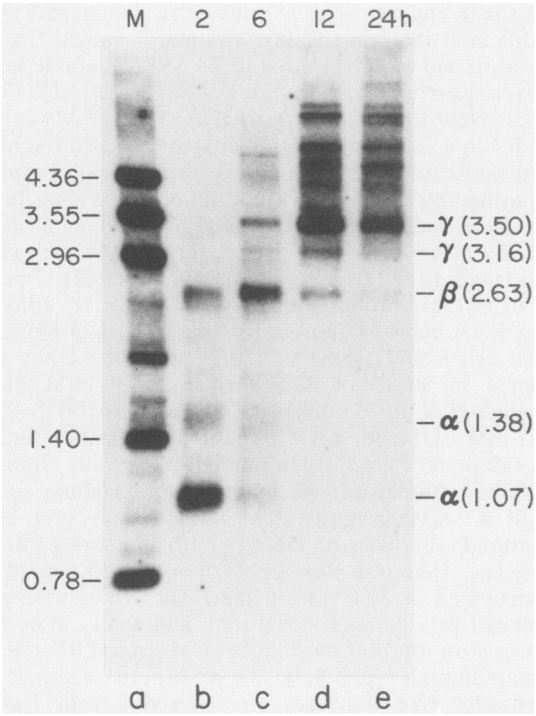

FIG. 1. Northern hybridization analysis of RNA homologous to AcNPV *Hin*dIII-K. Poly(A)-containing RNA isolated from 10^7 *Spodoptera frugiperda* cells 2, 6, 12, and 24 h after infection with AcNPV was glyoxalated and fractionated on a 1.7% agarose gel. The RNA was transferred to nitrocellulose and hybridized with the *Hin*dIII-K fragment (3.0 kb) cloned into pBR322 and radiolabeled with ^{32}P by nick translation. An autoradiogram (4-h exposure) is shown. Glyoxalated molecular weight standards derived from various restriction digests of the plasmid pBR322 are indicated (in kilobase pairs) at the left (lane a).

activation of increasingly larger transcripts making up the later classes accompanied by the coordinate turnoff of the smaller transcripts comprising the earlier classes.

To determine the approximate locations of the three temporal classes, RNA blots were hybridized with three nonoverlapping subclones of the *Hin*dIII-K fragment (Fig. 2). The results indicated that the early 1.07-kb and, on longer exposure, the minor 1.38-kb α transcript were only homologous to the rightmost P-H subclone (lane e). The 2.63-kb β transcript hybridized to all three subclones, but less intensely with the H-X subclone (lane c), localizing one of its ends within the left one-third of *Hin*dIII-K. Finally, the γ transcripts, including the major 3.50- and 3.16-kb RNAs (lanes c through e), spanned the entire region, overlapping the α and β RNAs. On longer exposures (lane b), each of the α, β, and γ transcripts was detected with the full-length *Hin*dIII-K clone. Thus, to various degrees, each temporal class of RNA was detected 12 h after infection. Northern blot analyses of various RNA preparations (data not shown) consistently demonstrated sequential activation of α, β, and γ RNAs; delays (≤6 h) in peak synthesis or shutoff of the different classes were occasionally observed, possibly the result of variations in culture conditions or multiplicity of infection.

***Hin*dIII-K RNA transcripts form an overlapping 3′ coterminal nest.** To determine the precise location and direction of transcription of the *Hin*dIII-K RNAs, we used the high-resolution S1 nuclease mapping procedure of Weaver and Weissman (38). Preliminary experiments indicated that transcription was from left to right. The 5′ ends of the β and γ transcripts were therefore mapped by hybridizing viral poly(A)$^+$ RNA with the leftmost 1.16-kb *Hin*dIII-*Xho*I fragment 5′ end labeled exclusively at the *Xho*I site (Fig. 3, panel A). Three S1-resistant DNA fragments (210, 790, and 1,160 bp) were resolved when the 5′ probe was hybridized to 12-h viral RNA (lane d). No fragments were observed when the same probe was hybridized to RNA from mock-infected cells (lane e). From these data and subsequent mapping of the 3′ termini (below), we concluded that the major 210-bp, the minor 790-bp, and the major 1,160-bp fragments correspond to the 5′ ends of the 2.63-kb β, the 3.16-kb γ, and the 3.50-kb γ transcripts, respectively. Further analysis (not shown) indicated that although the 3.50-kb γ transcript appears to span the leftmost *Hin*dIII site, it does not extend more than 40 bp in this direction.

The 5′ ends of the two α transcripts were mapped by hybridizing the rightmost 1.02-kb *Pst*I-*Hin*dIII fragment 5′ end labeled exclusively at the *Hin*dIII site (Fig. 3, panel B) with poly(A)$^+$ RNA isolated at 2, 6, and 12 h after infection. Three S1-resistant fragments were detected (lanes d through

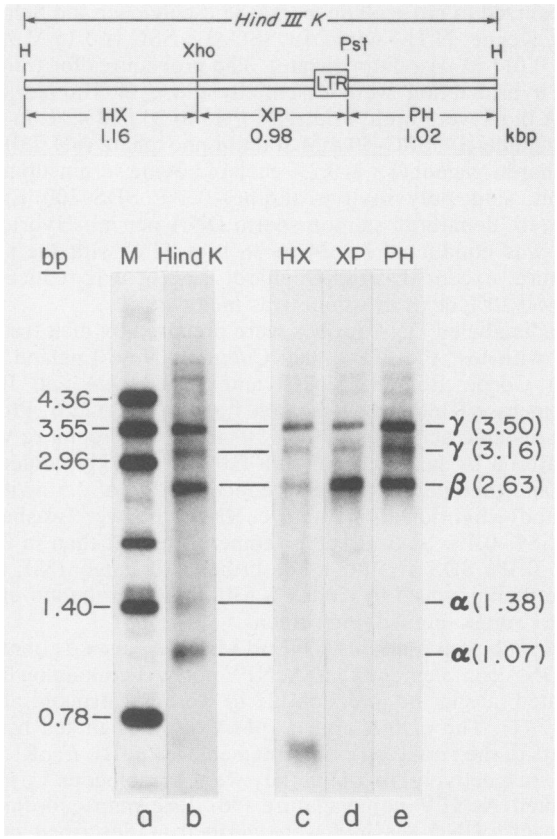

FIG. 2. Preliminary mapping of the *Hin*dIII-K RNA transcripts. Nitrocellulose blots of poly(A)-containing RNA isolated from cells 12 h after infection were hybridized with three nonoverlapping subclones of the *Hin*dIII-K fragment as shown. Lanes: c, leftmost *Hin*dIII-*Xho*I (HX) subclone; d, middle *Xho*I-*Pst*I (XP) subclone; and e, rightmost *Pst*I-*Hin*dIII (PH) subclone. Transcripts hybridizing with the full-length *Hin*dIII-K clone (lane b) are also indicated. Autoradiograms (3-h exposure; lanes c through e) with molecular weight standards (lane a) are shown. Subclones were derived from the *Hin*dIII-K fragment (3.3 kb) of the AcNPV insertion mutant FP-DS (top), which carries a 0.3-kb *copia*-like long terminal repeat (LTR) of host origin with a unique *Pst*I restriction site (26).

f). On the basis of these data and additional data presented below, we concluded that the prominent 440-bp fragment which decreased in intensity from 2 to 12 h after infection corresponded to the 5′ end of the major 1.07-kb α transcript, whereas the minor 830-bp fragment corresponded to that of the 1.38-kb α transcript. The 1,020-bp fragment increasing through 12 h resulted from the protection of the full-length 5′ probe (1.02 kb) by the β and γ transcripts spanning the region from left to right at these times. Finally, a 780-bp fragment was detected at 6 to 12 h (lanes e through f) and accounted for a very minor transcript (1.30 kb) that was detected only on long exposures of Northern blots. The 440-bp α-derived fragment was overrepresented relative to the 1,020-bp β- and γ-derived fragment (Fig. 3, panel B). This was indicated by additional analyses of the same RNA (data not shown), which demonstrated a dramatic decrease in the 440-bp α fragment and an increase in the 1,020-bp β and γ fragment when higher hybridization temperatures (46 to 50°C) were used. The locations of the 5′ termini of both α transcripts were confirmed by using a different 5′-end-labeled probe (*Eco*RI-*Hin*dIII, 0.84 kb) (see Fig. 6).

The sizes of the *Hin*dIII-K transcripts mapped above placed their 3′ termini close to one another within the adjacent *Hin*dIII-Q region (87.4 to 88.7 map units). We therefore localized these ends by using as a probe the 1.59-kb *Hin*dIII-*Xho*I fragment derived from *Hin*dIII-Q and 3′ end labeled exclusively at the leftmost *Hin*dIII site (Fig. 4, top). A single 540-bp S1-resistant fragment was observed (Fig. 4, bottom) when the 3′ probe was hybridized to poly(A)$^+$ RNA isolated 2, 6, and 12 h after infection (lanes d through f, respectively). No fragments were protected by mock-infected cell RNA (lane g). This indicated that each of the α, β, and γ transcripts terminated at a common 3′ site located 540 bp downstream from the *Hin*dIII-K/Q junction.

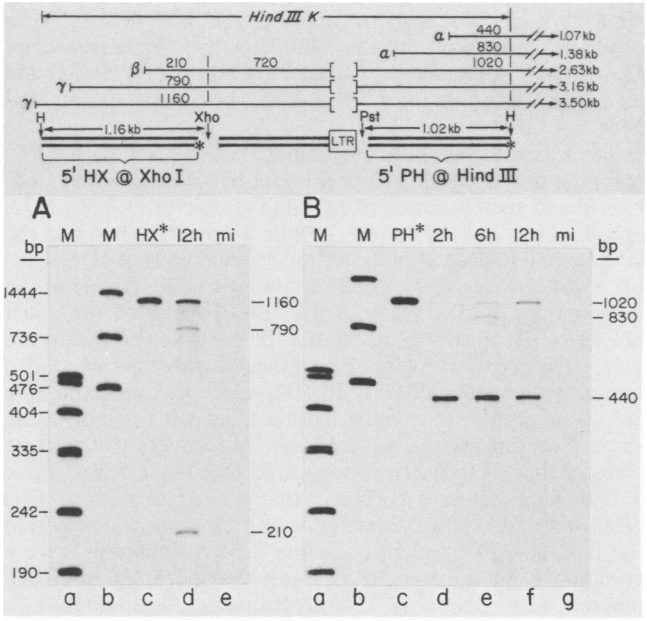

FIG. 3. S1 nuclease mapping of the 5′ ends of the *Hin*dIII-K RNA transcripts. Panel A: Mapping 5′ ends of the β and γ transcripts. Poly(A)-containing RNA (2 μg) isolated from cells 12 h after infection and RNA (2 μg) from mock-infected cells (mi) were hybridized at 50°C with 75 ng of the 1.16-kb *Hin*dIII-*Xho*I fragment 5′ end labeled exclusively at the *Xho*I site (see above diagram). *, Position of the 5′ label. The S1-resistant fragments generated from viral RNA 12 h after infection (lane d) and mock-infected RNA (lane e) were denatured and fractionated on a 4% acrylamide–7 M urea–TBE gel. An autoradiogram (6-h exposure) is shown. Panel B: Poly(A)-containing RNA (2 μg) was hybridized at 42°C with 75 ng of the 1.02-kb *Pst*I-*Hin*dIII fragment 5′ end labeled exclusively at the *Hin*dIII site (see diagram). The S1-resistant fragments generated from RNA isolated from cells 2 (lane d), 6 (lane e), and 12 h (lane f) after infection as well as mock-infected RNA (lane g) were analyzed as described above. An overexposed (36-h) autoradiogram is shown to enhance the minor fragments. Both panels include molecular weight standards (lanes a and b) and 5′-end-labeled DNA probes (HX* and PH*, respectively) before S1 treatment (lane c). The sizes of the S1-resistant fragments are indicated in base pairs (bp).

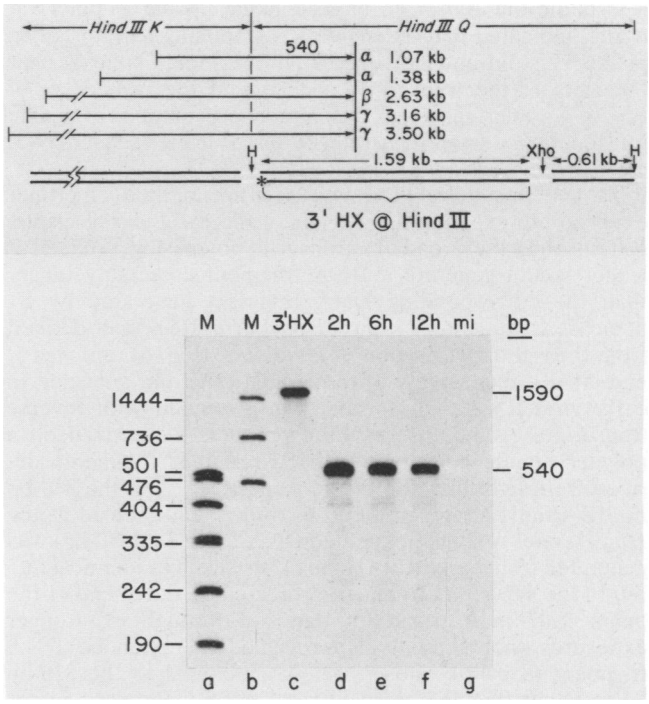

FIG. 4. Mapping the 3′ ends of the *Hin*dIII-K-related transcripts within fragment *Hin*dIII-Q. Samples (2 μg) of poly(A)-containing RNA from cells 2, 6, and 12 h after infection were hybridized at 50°C to 150 ng of the 1.59-kb *Hin*dIII-*Xho*I fragment 3′ end labeled exclusively at the *Hin*dIII site (see diagram). This probe was derived from the AcNPV *Hin*dIII-Q fragment cloned into plasmid pUC8. The S1-resistant fragments generated from viral RNA at 2 (lane d), 6 (lane e), and 12 h (lane f) after infection and mock-infected RNA (lane g) were fractionated on a 4% polyacrylamide–7 M urea–TBE gel. An autoradiogram (12-h exposure) with indicated molecular weight standards (lanes a and b) and the 3′ end-labeled DNA probe (3′ HX) before S1 treatment (lane c) is shown.

Figure 5 summarizes these data. The five *Hin*dIII-K transcripts formed an overlapping nest transcribed from left to right (5′ to 3′) on the AcNPV physical map. Although the 5′ ends extended upstream depending on time after infection, each RNA had a common 3′ end mapping immediately upstream from HR5 (6), a region of repetitive viral DNA with multiple *Eco*RI sites. Although the S1 nuclease data presented here accounted for all of the major *Hin*dIII-K transcripts which were 3.5 kb or smaller (Fig. 1), additional analysis indicated that the *Hin*dIII-K nest contains several other transcripts (4 to 6 kb) whose 5′ ends extended even further upstream into the adjacent *Hin*dIII-B_2 region (data not shown).

Primer extension analysis of the 5′ terminus of the α transcripts. The exact correlation between sizes of the S1-resistant hybrids and the corresponding *Hin*dIII-K RNAs

[excluding the 100 or so bases making up the 3′ poly(A)$^+$ tracts] indicated that extensive RNA splicing had not taken place. This did not, however, rule out limited splicing near the ends of the transcripts occurring if the nested set of RNAs was derived from a common precursor responsible for donating a small (less than 50 bp) 5′ leader sequence (3, 4).

To test this possibility, we used the method of primer extension to examine the 5′ ends of the early α transcripts. Extension to the 5′ end of a transcript possessing a spliced 5′ leader would generate a DNA fragment detectably longer than the corresponding DNA fragment generated by S1 nuclease treatment. A 390-bp *Hpa*II-*Hin*dIII primer derived from the rightmost portion of *Hin*dIII-K (Fig. 6, top) was 5′ end labeled exclusively at the *Hin*dIII site and annealed to early viral RNA. This primer was extended with reverse transcriptase, and the resulting products were sized on a polyacrylamide gel along with S1-resistant fragments derived from hybridization of the same RNA with the 840-bp *Eco*RI-*Hin*dIII fragment (Fig. 6, top) 5′ end labeled at the *Hin*dIII site. A single, extended DNA fragment (442 bp) was generated from early RNA (lane f). Its size was identical (±5 bp) to the 442-bp S1 fragment protected by the 5′ end of the major 1.07-kb α transcript (lanes d through e). Longer exposures (not shown) also revealed an extended DNA fragment (830 bp) whose size was identical to the 830-bp S1-resistant fragment derived from the 5′ end of the minor 1.38-kb α transcript. That the extension assay was capable of detecting 5′ ends located at least 600 bp farther upstream from the primer was demonstrated by the presence of an additional extended fragment (1,050 bp) when primer was annealed to RNA isolated from cells infected with the AcNPV-mutant FP-DS (lane g). FP-DS transcribes an abundant RNA (1.68 kb) whose 5′ end maps 1.0 kb upstream from the *Hin*dIII-K/Q junction (manuscript in preparation). No extension products were detected when primer was annealed to yeast tRNA (lane h). Since the size of the extended primer coincided with that of the 5′ end of the 1.07- and 1.38-kb α transcripts identified by S1 nuclease analysis, it was concluded that these RNAs do not possess 5′ leaders (greater than 5 bp) derived from splicing of noncontiguous sequences.

Temporal regulation of overlapping RNA transcripts within the *Hin*dIII-A/*Eco*RI-C regions. To search other regions of the AcNPV genome for overlapping RNAs under temporal regulation, poly(A)$^+$ RNA blots were hybridized with recombinant clones of DNA complementary to mRNAs isolated late (27 h) after infection (1). The cDNA clones were designated by the letters of the AcNPV restriction fragments to which they were homologous (see above). The use of these cDNA probes ensured that the RNAs detected were indeed overlapping, transcribed from either the same or opposite DNA strands.

Two adjacent cDNA clones from the *Hin*dIII-A/*Eco*RI-C region (43.2 to 52.9 map units) revealed overlapping patterns of both early and late RNAs (Fig. 7). The pattern generated by cDNA ACD (left panel) exhibited an activation of sequentially larger transcripts with time, accompanied by the deactivation of earlier small transcripts in a manner remarkably similar to that of the *Hin*dIII-K region. First to appear was the smallest transcript (0.92 kb), from 2 to 6 h, followed by a 2.04-kb transcript from 6 to 12 h and finally by the largest transcripts (3.24, 3.76, and 4.95 kb) from 6 to 24 h with peak synthesis at 12 h after infection.

The complex pattern generated by cDNA ACG (Fig. 7, right panel), on the other hand, revealed several small transcripts (1.22, 1.93, and 2.14 kb) which were activated early (6 h) yet continued to accumulate through 24 h. Several high-molecular-weight transcripts (3.09, 3.39, 3.76, and 4.95 kb) exhibited maximum synthesis at 12 h but declined by 24 h. The 3.76- and 4.95-kb transcripts also hybridized to cDNA ACD (left panel), which suggested that the two sets of RNAs are located within 3 to 4 kb of one another. The detailed organization of these two transcription units remains to be established.

Overlapping RNAs transcribed from major late AcNPV genes: p10 and polyhedrin. In sharp contrast to the above regions, cDNA clones of the p10 and polyhedrin genes revealed overlapping patterns of RNAs with maximum synthesis during the very late occlusion phase (δ). cDNA P(Q)P (p10 cDNA), a clone homologous to the late AcNPV gene p10 previously mapped to the *Hin*dIII-Q/P junction (88.7 map units) (1) detected four transcripts (0.72, 2.56, 2.72, and 4.68 kb) (Fig. 8, right panel). The most abundant transcript (0.72 kb), first appearing at 12 h and accumulating rapidly through 24 h after infection, represented the mRNA for p10, an abundant nonstructural protein (10,000 daltons) synthesized from 15 to 60 h after infection (1, 28–30). The p10 mRNA is transcribed from left to right (Fig. 8, bottom) (1, 20, 31). The abundant 2.56- and 2.72-kb transcripts appeared simultaneously with the p10 mRNA and accumulated at similar rates. No early α or β (2- to 6-h) RNAs were observed. In addition to the p10 mRNA, a single transcript (2.6 kb) was detected in this region by others (19, 29, 31) and probably represents the 2.56- and 2.72-kb RNA pair detected here.

An adjacent but nonoverlapping late cDNA clone PB, mapping downstream within the *Hin*dIII-P/*Eco*RI-B region, hybridized to the larger p10-related transcripts (2.56, 2.72, and 4.68 kb) above, a new 1.78-kb transcript, but not the 0.72-kb p10 mRNA (Fig. 8, left panel). Given that cDNA PB (0.28 kb) was derived by oligothymidylic acid priming at the 3′ terminus of a single mRNA, the 3′ end of the most abundant PB transcript (2.56 or 2.72 kb) mapped within the *Hin*dIII-P/*Eco*RI-B region. Since these transcripts were also homologous to the p10 [P(Q)P] cDNA located approximately 2.5 kb upstream, they must extend from left to right in the same direction as the p10 mRNA. Moreover, the relative sizes of the PB transcripts suggested that these RNAs have 5′ ends identical to or very near that of the p10 mRNA. This was confirmed by a recent report which demonstrated that the 0.72-kb p10 transcript and the 2.6-kb transcript have a common 5′ end located 300 bp to the left of the *Hin*dIII-Q/P junction (20). The new 1.78-kb transcript, homologous to cDNA PB and synthesized late (12 to 24 h), did not overlap the p10 sequences of cDNA P(Q)P (Fig. 8) and must therefore be initiated from a different promoter within the region. The direction of transcription of this RNA remains to be determined.

Transcriptional analysis of the late viral gene for polyhedrin, a major protein component (28,872 daltons) of viral occlusion bodies, revealed a similar pattern of overlapping transcripts (Fig. 9). cDNA VI, mapping to the *Hin*dIII-V/*Eco*RI-I region (3.3 map units) (1) and carrying the 3′ terminal sequences of polyhedrin, hybridized most prominently to the polyhedrin mRNA (1.28 kb). This transcript was observed as early as 6 h, even though intracellular synthesis of polyhedrin has not been detected before 12 to 15 h after infection (5, 32, 39; unpublished results). Two other abundant transcripts (3.39 and 4.9 kb) were synthesized with kinetics identical to that of the 1.28-kb mRNA and were detected earlier (19, 29, 31). Subsequent mapping by North-

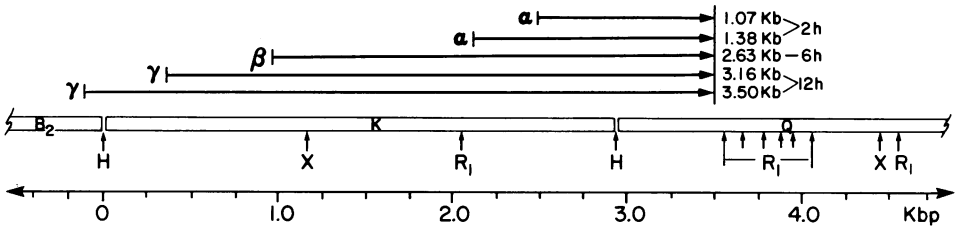

FIG. 5. Transcriptional map of the AcNPV *Hin*dIII-K region. The five poly(A)-containing RNAs were transcribed in the same direction (left to right, 5′ to 3′) and terminated at a common 3′ site located 540 bp downstream from the *Hin*dIII-K/Q junction (87.4% of the AcNPV genome). Sizes of the various transcripts and their period of maximum accumulation (2, 6, and 12 h postinfection) are indicated. The scale at the bottom illustrates the size (kbp) of the region.

ern hybridization revealed that the 3.39- and 4.9-kb transcripts extended downstream from the polyhedrin gene (Fig. 9, bottom), since both were homologous to the adjacent *Hin*dIII-T fragment but not the *Sal*I-*Eco*RV fragment located 35 bp upstream of the 5′ end of the 1.28-kb polyhedrin mRNA (data not shown). A single RNA start site has been mapped to the region between the *Eco*RV site and the *Hin*dIII-F/V junction (14, 31). These data are consistent with a model that these transcripts initiate at a 5′ site identical to the polyhedrin mRNA but terminate at 3′ sites farther downstream in the *Eco*RI-R region. Mapping the 3′ ends of these transcripts should confirm this model.

DISCUSSION

To gain insight into the mechanisms used by large DNA viruses to regulate gene expression, we have analyzed the

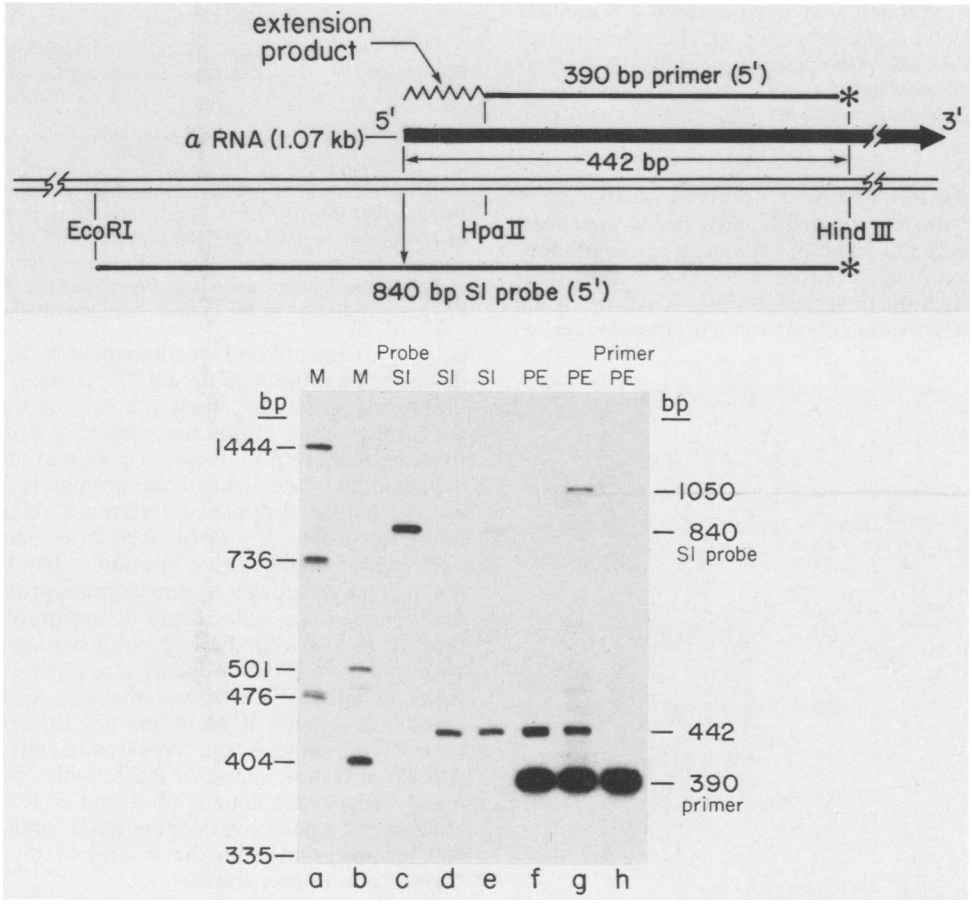

FIG. 6. Primer extension mapping of the 5′ termini of the early α transcripts. Poly(A)-containing RNA (2 μg) from AcNPV-infected cells (lane f), FP-DS mutant-infected cells (lane g), and 2 μg of tRNA (lane h) were annealed to 5 ng of the 390-bp *Hpa*II-*Hin*dIII primer 5′ end labeled exclusively at the *Hin*dIII site (see top diagram) and extended with reverse transcriptase. An autoradiogram (5-h exposure) of a 4% polyacrylamide–7 M urea gel used to fractionate the products by size is shown. S1-resistant fragments generated from the hybridization of 2 μg of poly(A)$^+$ RNA from cells 2 (lane d) and 6 h (lane e) after infection with 100 ng of the 840-bp *Eco*RI-*Hin*dIII probe 5′ end labeled exclusively at the *Hin*dIII site (see diagram) were fractionated on the same gel. Molecular weight standards (lanes a and b) and the 5′-labeled *Eco*RI-*Hin*dIII probe before S1 treatment (lane c) are included.

temporal synthesis and organization of RNA transcripts in several regions of the genome of the insect baculovirus, *Autographa californica* NPV. Of 10 regions examined thus far, 6 presented here, each contained 2 to 12 overlapping RNAs. Two distinct transcriptional patterns were observed; the first comprised both early and late RNAs having a common 3′ end and the second comprised only very late RNAs having extended 3′ ends.

Temporal regulation within an overlapping 3′ coterminal nest of RNAs. The five transcripts (1.07 to 3.50 kb) mapped to the *Hin*dIII-K region formed an overlapping group of RNAs, all transcribed in the same direction (left to right or clockwise on the circular AcNPV map) and terminated at a common 3′ site (Fig. 5). Although similar 3′ coterminal patterns have been documented for other large DNA viruses, including vaccinia, herpes simplex virus, and adenovirus (3, 12, 21, 37), the AcNPV *Hin*dIII-K nest represented one of the more striking examples of the coordinate regulation of overlapping immediate early (α), early (β), and late (γ) genes (Fig. 1).

We initially speculated that this pattern, exhibiting a sequential replacement of early transcripts with longer transcripts initiated farther upstream, was the result of a temporally regulated splicing process. S1 nuclease mapping, however, revealed no evidence for splicing of early or late *Hin*dIII-K RNAs, a conclusion corroborated by another study (19) which found no evidence for splicing of major late (24-h) AcNPV RNAs. Moreover, primer extension analysis (Fig. 6) ruled out the possibility of limited splicing near the 5′ ends of the two α transcripts (1.07 and 1.38 kb) and suggested rather that each of these RNAs was transcribed from a unique promoter.

Since both early α RNAs were not derived via splicing of a larger precursor, the 5′-extended β and γ RNAs appearing later in infection were the result of activation of one or more promoters upstream of the α promoters. This is consistent with a model in which the observed *Hin*dIII-K pattern is the result of sequential activation of upstream promoters (i.e., α, β, and γ, respectively), accompanied by the deactivation of downstream promoters (α and β). As such, this model raises interesting questions about the role of the host and viral RNA polymerase (10) in the sequential activation and deactivation of these promoters. A potential mechanism for the deactivation of the downstream promoters involves a type of *cis*-acting transcriptional interference referred to as "promoter occlusion" (2). RNA polymerase molecules initiating upstream at highly active promoters block access of RNA polymerase molecules to downstream promoters by way of steric hinderance or localized distortion of the DNA structure. At least two preliminary observations were consistent with this model: (i) in repetitive analyses, the amount of α RNA in infected cells was inversely proportional to the amount of β and γ RNA at any one time (data not shown); (ii) α RNA synthesis was repressed in cells infected with the AcNPV-insertion mutant, FP-DS, which synthesized significantly reduced amounts of β and γ RNA but abundant amounts of a new, overlapping RNA whose 5′ end mapped 600 bp upstream from the 5′ end of the 1.07-kb α RNA (manuscript in preparation).

The 5′ extended arrangement of the *Hin*dIII-K RNAs suggested that the longer and later transcripts might therefore serve a dual purpose: first, to repress transcription of earlier genes located downstream, and second, to act as mRNAs for late viral products. Indeed, the dramatic turning on and off of these RNAs (Fig. 1) suggested that a primary function of this region was to provide for the highly regu-

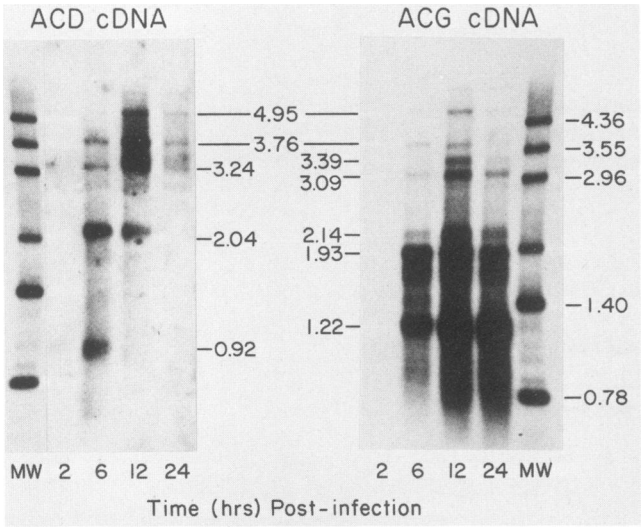

FIG. 7. Northern hybridization of RNA homologous to cDNAs ACD and ACG. Nitrocellulose blots of poly(A)-containing RNA isolated from cells 2, 6, 12, and 24 h after infection as described in the legend to Fig. 1 were hybridized to radiolabeled cDNA plasmids pMA-ACD (left) and pMA-ACG (right). Autoradiograms (24- and 4-h exposures, left and right, respectively) with molecular weight standards (MW) are shown.

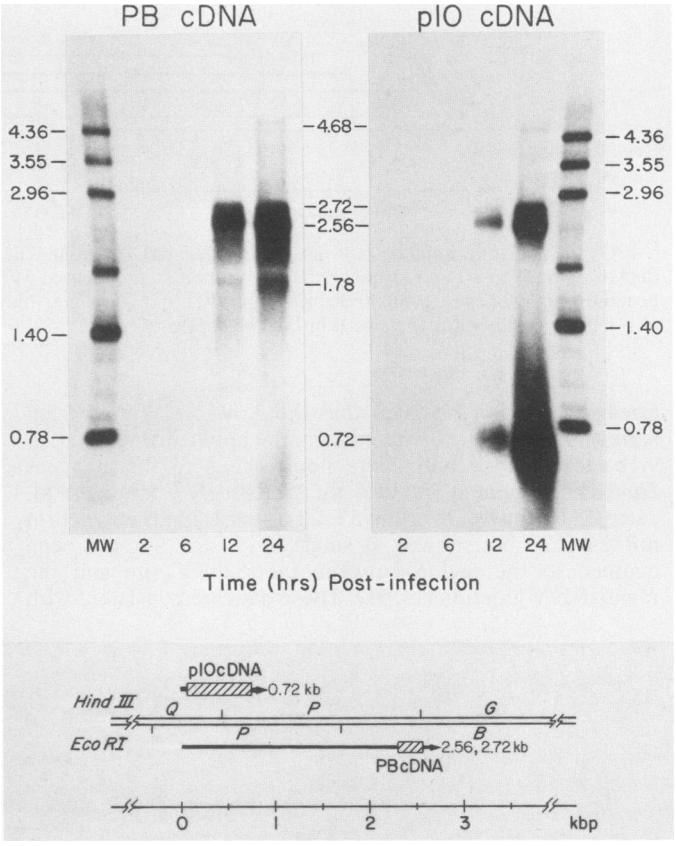

FIG. 8. Northern hybridization of RNA homologous to cDNAs PB and P(Q)P (p10). RNA blots were hybridized with radiolabeled cDNA plasmids pMA-PB (left) and pMA-P(Q)P (right). Autoradiograms (4-h exposures) are shown. Bottom: organization of major PB and p10 overlapping transcripts. Positions of cDNA clones PB (0.28 kb) and p10 (0.60 kb) are indicated by the shaded boxes.

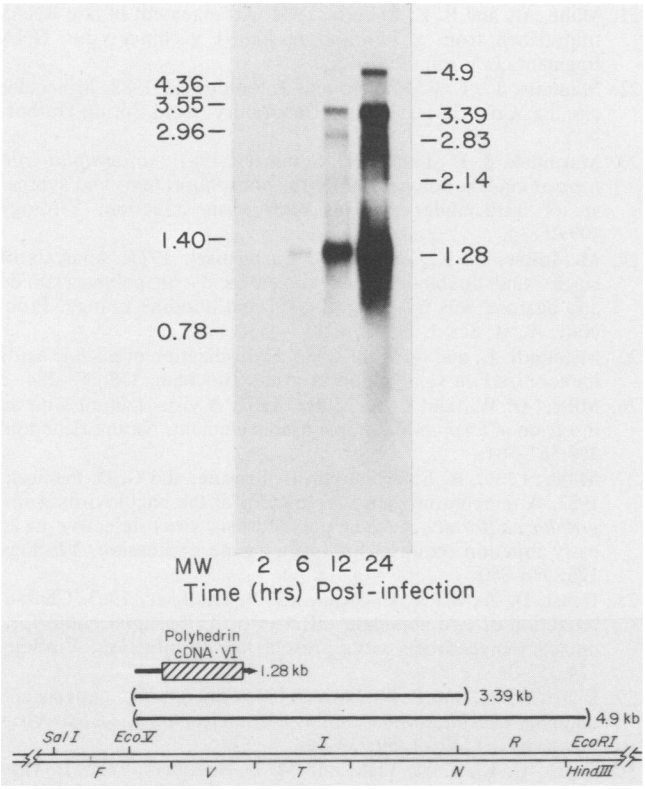

FIG. 9. Northern hybridization of RNA homologous to polyhedrin cDNA VI. Poly(A)-containing RNA was transferred to nitrocellulose as described in Fig. 1 and hybridized with cDNA plasmid pMA-VI. An autoradiogram (4-h exposure) is shown. Bottom: proposed model for the organization of overlapping RNA transcripts within the *Hin*dIII-V/*Eco*RI-I region. The 1.28-kb polyhedrin mRNA is transcribed left to right (5′ to 3′), initiating 35 bp downstream from the *Eco*RV site and extending approximately 1,200 bp downstream to the *Hin*dIII-V/T junction (14). The shaded box indicates the position of the VI cDNA clone (0.74 kb).

lated synthesis of at least three viral products (i.e., α, β, and γ). In vitro translation studies should help identify the viral polypeptides encoded by this region and, in particular, those synthesized from the potentially polycistronic β and γ RNAs.

Lastly, the above type of transcriptional regulation and organization was not limited to the *Hin*dIII-K region. Although the arrangement of the overlapping RNAs detected by cDNA ACD (Fig. 7, panel A) remains to be determined, their regulation involved a similar activation of successively longer RNAs and a deactivation of earlier small RNAs. Recently, two transcription nests consisting of overlapping RNAs with a common 3′ end have also been mapped to the *Hin*dIII-I/*Eco*RI-F and the *Hin*dIII-B_2/*Eco*RI-H regions of AcNPV (20). Moreover, cDNA-Northern blot analysis of the RNAs within both of these regions has revealed a sequential activation of early, small RNAs followed by longer RNAs mapping further upstream (T. Mainprize and L. K. Miller, unpublished results). These transcription units represent additional candidates for testing the proposed model for sequential promoter activation.

Regulation of overlapping late (δ) transcripts. The abundantly expressed AcNPV genes, p10 and polyhedrin, were each transcribed by several overlapping RNAs with peak synthesis during the very late occlusion phase (δ) from 15 to 60 h after infection. In sharp contrast to the transcripts of the *Hin*dIII-K and *Hin*dIII-A/*Eco*RI-C regions, no early RNAs were detected. The p10 and polyhedrin units were each composed of a small, very abundant RNA and several longer, less abundant RNAs, all transcribed with identical kinetics. Our data, based on the map positions of cDNAs constructed from the 3′ ends of poly(A)-containing transcripts, indicated that the p10 unit was composed of RNAs with 3′ extended ends. Furthermore, recent S1 nuclease mapping has demonstrated that these RNAs have a common 5′ end (20). Similarly, the 3.39- and 4.9-kb transcripts (Fig. 9) which overlapped the major polyhedrin mRNA (1.28 kb) extended downstream apparently from a common 5′ site, also consistent with previous mapping (31). The coordinate regulation of RNAs within both units of transcription supported the contention that each overlapping RNA is transcribed from a common promoter.

The functional significance of the 3′ extended transcriptional units is not yet clear. A question to be resolved is whether these RNAs represent messengers for identical or different viral polypeptides. cDNA VI hybrid selected mRNA which directed the cell-free synthesis of polyhedrin and minor amounts of polyhedrin-related polypeptides (1), suggesting that the longer VI transcripts were either messenger inactive in the rabbit reticulocyte system or were also translated into polyhedrin. A single open reading frame with the predicted polyhedrin sequence has been identified immediately downstream from the 5′ ends of these transcripts (14). On the other hand, cDNA PB homologous to the two larger p10-related transcripts (2.56 and 2.72 kb) but not the major p10 mRNA (0.72 kb) hybrid selected mRNA which synthesized three proteins, of 30,000, 31,000, and 52,000 daltons, respectively (1). Given that another transcript (1.78 kb) overlaps this region (Fig. 8), these proteins could not be assigned to a specific messenger. It was not apparent whether the larger p10-related mRNAs also directed the synthesis of p10, since this polypeptide was not radiolabeled with the [^{35}S]methionine used.

The longer RNAs of each unit are apparently derived from readthrough of termination signals at the 3′ end of the smallest RNA. Unlike late vaccinia virus transcripts with heterogeneous 3′ ends (21), these late AcNPV transcripts terminate at defined sites, since RNAs of discrete sizes were observed. The contrasting lack of readthrough at the 3′ end of the *Hin*dIII-K nest even late during infection (Fig. 4) suggested that p10 and polyhedrin readthrough may be a function of the termination sequences themselves rather than a modification of the termination process.

Finally, the 3′ extended polyhedrin RNAs may play a role in the suppression of transcription of early viral genes located downstream via promoter occlusion. The extended polyhedrin-related transcripts, in particular, overlap smaller transcripts within the downstream *Hin*dIII-T and *Hin*dIII-N regions (unpublished data); this raises the interesting possibility of *cis*-acting regulation between adjacent transcriptional units.

ACKNOWLEDGMENTS

We thank Martin R. Hodge for excellent technical assistance throughout the course of this project. We also thank David W. Miller and Kumar Srinivasan for kindly providing AcNPV and FP-DS recombinant DNA clones.

This research was supported in part by Public Health Service grant AI 17338 from the National Institute of Allergy and Infectious Diseases and by a grant from the University of Idaho Research Council.

LITERATURE CITED

1. **Adang, M. J., and L. K. Miller.** 1982. Molecular cloning of DNA complementary to mRNA of the baculovirus *Autographa cali-*

fornica nuclear polyhedrosis virus: location and gene products of RNA transcripts found late in infection. J. Virol. **44**:782–793.
2. **Adhya, S., and M. Gottesman.** 1982. Promoter occlusion: transcription through a promoter may inhibit its activity. Cell **29**:939–944.
3. **Berget, S. M., C. Moore, and P. Sharp.** 1979. Spliced segments at the 5′ terminus of Ad 2 late mRNA. Proc. Natl. Acad. Sci. U.S.A. **74**:3171–3175.
4. **Berk, A. J., and P. A. Sharp.** 1977. Sizing and mapping of early adenovirus mRNAs by gel electrophoresis of S1 endonuclease-digested hybrids. Cell **12**:721–732.
5. **Carstens, E. B., S. T. Tjia, and W. Doerfler.** 1979. Infection of *Spodoptera frugiperda* cells with *Autographa californica* nuclear polyhedrosis virus. Virology **99**:386–398.
6. **Cochran, M. A., and P. Faulkner.** 1983. Location of homologous DNA sequences interspersed at five regions in the baculovirus AcMNPV genome. J. Virol. **45**:961–970.
7. **Dobos, P., and M. A. Cochran.** 1980. Protein synthesis in cells infected by *Autographa californica* nuclear polyhedrosis virus (AcNPV): the effect of cytosine arabinoside. Virology **103**: 446–464.
8. **Erlandson, M. A., and E. B. Carstens.** 1983. Mapping early transcription products of *Autographa californica* nuclear polyhedrosis virus. Virology **126**:398–402.
9. **Esche, H., H. Lübbert, B. Siegmann, and W. Doerfler.** 1982. The translation map of the *Autographa californica* nuclear polyhedrosis virus (AcNPV) genome. EMBO J. **1**:1629–1633.
10. **Fuchs, L. Y., M. S. Woods, and R. F. Weaver.** 1983. Viral transcription during *Autographa californica* nuclear polyhedrosis virus infection: a novel RNA polymerase induced in infected *Spodoptera frugiperda* cells. J. Virol. **48**:641–646.
11. **Gardiner, G. R., and H. Stockdale.** 1975. Two tissue culture media for production of lepidopteran cells and nuclear polyhedrosis viruses. J. Invertebr. Pathol. **25**:363–370.
12. **Golini, F., and J. R. Kates.** 1984. Transcriptional and translational analysis of a strongly expressed early region of the vaccinia viral genome. J. Virol. **49**:459–470.
13. **Holmes, D. S., and M. Quigley.** 1981. A rapid method for the preparation of bacterial plasmids. Anal. Biochem. **114**:193–197.
14. **Hooft van Iddekinge, B. J. L., G. E. Smith, and M. D. Summers.** 1983. Nucleotide sequence of the polyhedrin gene of *Autographa californica* nuclear polyhedrosis virus. Virology **131**:561–565.
15. **Hruby, D. E., and W. K. Roberts.** 1976. Encephalomyocarditis virus RNA: variations in polyadenylic acid content and biological activity. J. Virol. **19**:325–330.
16. **Kelly, D. C.** 1982. Baculovirus replication. J. Gen. Virol. **63**:1–13.
17. **Kelly, D. C., and T. Lescott.** 1981. Baculovirus replication: protein synthesis in *Spodoptera frugiperda* cells infected with *Trichoplusia ni* nuclear polyhedrosis virus. Microbiologica **4**:35–57.
18. **Lee, H. H., and L. K. Miller.** 1978. Isolation of genotypic variants of *Autographa californica* nuclear polyhedrosis virus. J. Virol. **27**:754–767.
19. **Lübbert, H., and W. Doerfler.** 1984. Mapping of early and late transcripts encoded by the *Autographa californica* nuclear polyhedrosis virus genome: is viral RNA spliced? J. Virol. **50**:497–506.
20. **Lübbert, H., and W. Doerfler.** 1984. Transcription of overlapping sets of RNAs from the genome of *Autographa californica* nuclear polyhedrosis virus: a novel method for mapping RNAs. J. Virol. **52**:255–265.
21. **Mahr, A., and B. E. Roberts.** 1984. Arrangement of late RNAs transcribed from a 7.1-kilobase *Eco*RI vaccinia virus DNA fragment. J. Virol. **49**:510–520.
22. **Maniatis, T., E. F. Fritsch, and J. Sambrook.** 1982. Molecular cloning. Cold Spring Harbor Laboratory, Cold Spring Harbor, N.Y.
23. **Maruniak, J. E., and M. D. Summers.** 1981. *Autographa californica* nuclear polyhedrosis virus phosphoproteins and synthesis of intracellular proteins after virus infection. Virology **109**:25–34.
24. **McMaster, G. K., and G. G. Carmichael.** 1977. Analysis of single- and double-stranded nucleic acids on polyacrylamide and agarose gels by using glyoxal and acridine orange. Proc. Natl. Acad. Sci. U.S.A. **74**:4835–4838.
25. **Meinkoth, J., and G. Wahl.** 1984. Hybridization of nucleic acids immobilized on solid supports. Anal. Biochem. **138**:267–284.
26. **Miller, D. W., and L. K. Miller.** 1982. A virus mutant with an insertion of a *copia*-like transposable element. Nature (London) **299**:562–564.
27. **Miller, L. K., R. E. Trimarchi, D. Browne, and G. D. Pennock.** 1983. A temperature sensitive mutant of the baculovirus *Autographa californica* nuclear polyhedrosis virus defective in an early function required for further gene expression. Virology **126**: 376–380.
28. **Rohel, D. Z., M. A. Cochran, and P. Faulkner.** 1983. Characterization of two abundant mRNAs of *Autographa californica* nuclear polyhedrosis virus present late in infection. Virology **124**:357–365.
29. **Rohel, D. Z., and P. Faulkner.** 1984. Time course analysis and mapping of *Autographa californica* nuclear polyhedrosis virus transcripts. J. Virol. **50**:739–747.
30. **Smith, G. E., J. M. Vlak, and M. D. Summers.** 1982. In vitro translation of *Autographa californica* nuclear polyhedrosis virus early and late mRNAs. J. Virol. **44**:199–208.
31. **Smith, G. E., J. M. Vlak, and M. D. Summers.** 1983. Physical analysis of *Autographa californica* nuclear polyhedrosis virus transcripts for polyhedrin and 10,000-molecular-weight protein. J. Virol. **45**:215–225.
32. **Summers, M. D., L. E. Volkman, and C. Hsiech.** 1978. Immunoperoxidase detection of baculovirus antigens in insect cells. J. Gen. Virol. **40**:545–557.
33. **Thomas, P. S.** 1980. Hybridization of denatured RNA and small DNA fragments transferred to nitrocellulose. Proc. Natl. Acad. Sci. U.S.A. **77**:5201–5205.
34. **Vaughn, J. L., R. H. Goodwin, G. L. Thompkins, and P. McCawley.** 1977. Establishment of two insect cell lines from the insect *Spodoptera frugiperda* (Lepidoptera: Noctuidae). In Vitro **13**:213–217.
35. **Vieira, J., and J. Messing.** 1982. The pUC plasmids, an M13mp7-derived system for insertion mutagenesis and sequencing with universal primers. Gene **19**:259–268.
36. **Vlak, J. M., and G. E. Smith.** 1982. Orientation of the genome of *Autographa californica* nuclear polyhedrosis virus: a proposal. J. Virol. **41**:1118–1121.
37. **Wagner, E. K.** 1983. Transcriptional patterns in HSV infections. Adv. Viral Oncol. **3**:239–270.
38. **Weaver, R. F., and C. Weissman.** 1979. Mapping of RNA by a modification of the Berk-Sharp procedure: the 5′ termini of 15S β-globin mRNA precursor and mature 10S β-globin mRNA have identical map coordinates. Nucleic Acids Res. **7**:1175–1193.
39. **Wood, H. A.** 1979. *Autographa californica* nuclear polyhedrosis virus-induced proteins in tissue culture. Virology **102**:21–27.